

Concerning the heat and mass transfer features on permeable surfaces

E.P. Volchkov *

Kutateladze Institute of Thermophysics, Siberian Branch of Russian Academy of Sciences, 630090 Novosibirsk, Russia

Received 20 February 2005; received in revised form 14 June 2005

Available online 19 October 2005

Abstract

For a boundary layer above the porous surface at a given temperature of main flow and injected gas, the wall heat flux q_w depends on the injection intensity in nonmonotonic way. The heat flux first increases with the growth in injection rate j_w , then after reaching a maximum it starts decreasing and tends to zero at $j_w \rightarrow j_{cr}$. The similarity problem between heat and mass transfer is considered for boundary layers with variable content. The effect of the Lewis number Le on similarity conditions was demonstrated. In general case, the similarity ratio is a function not only Lewis number, but also the enthalpy difference. The common formula for description of similarity $St_T Le^n = St_D$ “works” only for specific cases. Results on the influence of flow acceleration and turbulence degree Tu on characteristics of a boundary layer with combustion are presented.

© 2005 Elsevier Ltd. All rights reserved.

1. Influence of boundary conditions on heat and mass transfer on a porous surface

Processes of heat and mass transfer on porous surfaces are of interest for different technical applications: porous cooling, evaporation, condensation, combustion, absorption, etc.

In most of theoretical papers the effect of gas injection on heat transfer is usually analyzed at a constant wall temperature $T_w = \text{const}$ for the entire range of injection parameter $0 < b < b_{cr}$ (e.g., in [1–3]). However, this boundary condition does not satisfy the limiting cases: for injection parameter $b \rightarrow 0$ the wall temperature tends to the temperature of mainstream $T_w \rightarrow T_0$, and for critical injection $b \rightarrow b_{cr}$ the wall temperature T_w have to approach the temperature of injected gas $T_w \rightarrow T'$. Besides, at given $T_0 = \text{const}$ and $T_w = \text{const}$, with a change in injection parameter, the injected gas temperature also varies. The estimates from the conditions at $j_w \rightarrow 0$ give almost unreal-

istic negative values. Solutions of this kind indicate that the heat transfer coefficient (Stanton number) and heat flux to the wall are maximal at zero injection and they decrease smoothly with growth in the injection flow rate. That is why a kind of stereotype was cast that the higher injection means a decrease in heat flux and a fall in parameter gradients (velocity, temperature, concentration) on the wall.

However, from the physical and practical points of view, we have the given parameters for the main stream and injected gas; the temperature of the main flow $T_0 = \text{const}$ and injected gas $T' = \text{const}$ are prescribed and constant. The wall temperature only can be obtained within this range $T' < T_w < T_0$.

Here we consider several features of heat and mass transfer in a laminar boundary layer with injection at given parameters of the main and injected flow $T_0 = \text{const}$, $T' = \text{const}$. The approximate analytical analysis is given and numerical solutions for differential equations of a boundary layer are presented. Consider the heat balance on a porous wall

$$q_w = \left(-\lambda \cdot \frac{\partial T}{\partial y} \right)_w = j_w \cdot C'_p \cdot (T_w - T') \quad (1)$$

* Tel.: +7 3832 342008; fax: +7 3832 343480.

E-mail address: volchkov@itp.nsc.ru

Nomenclature

$C_f/2$	friction coefficient
C_p	heat capacity at constant pressure, J/(kg K)
D	diffusion coefficient of a substance, m ² /s
K_i	mass concentration of the <i>i</i> th component of mixture
Le	Lewis number
M	gas molecular mass, kg/kmol
P	pressure, N/m ²
Pr	Prandtl number
Re	Reynolds number
Sc	Schmidt number
St	Stanton number
T	temperature, K
Tu	turbulence degree
U, V	projections of velocity vector to directions <i>x</i> and <i>y</i> , m/s
b	permeability parameter for the surface (calculated via Stanton number)

h	enthalpy, J/kg
$j = \rho \cdot V$	transversal mass flux, kg/(m s)
k	parameter of flow acceleration
q	heat flux density, J/(m ² s)
x, y	coordinates, m
Ψ	relative function of heat transfer
λ	thermal conductivity, J/(m s K)
μ	dynamic viscosity, (N s)/m ²
ν	kinematic viscosity, m ² /s
ρ	density, kg/m ³
τ	shear stress, N/m ²

Subscripts and superscripts

0	parameters of the main stream
'	parameters of injected gas
w	wall conditions
cr	critical parameters

and definition for the Stanton number

$$St = \frac{q_w}{\rho_0 \cdot U_0 \cdot C_{p0} \cdot (T_0 - T_w)} \quad (2)$$

This gives us the relationships:

$$T_w - T' = \frac{q_w}{j_w \cdot C_p'}; \quad T_0 - T_w = \frac{q_w}{\rho_0 \cdot U_0 \cdot C_{p0} \cdot St} \quad (3)$$

By adding these relationships termwise, we obtain

$$T_0 - T' = q_w \cdot \left(\frac{1}{j_w \cdot C_p'} + \frac{1}{\rho_0 \cdot U_0 \cdot C_{p0} \cdot St} \right) \text{ or} \quad (4)$$

$$\bar{q}_w = \frac{q_w}{\rho_0 \cdot U_0 \cdot C_{p0} \cdot (T_0 - T')} = \frac{1}{\frac{\rho_0 \cdot U_0 \cdot C_{p0}}{j_w \cdot C_p'} + \frac{1}{St}}$$

The dimensionless heat flux in the left side of this formula is an analog of Stanton number, but instead of temperature difference $\Delta T = T_0 - T_w$ we introduce the difference $T_0 - T'$, which is given and constant. Let us introduce the relative function of heat transfer $\Psi = (St/St_0)$, where St_0 is the Stanton number on an impermeable wall for the same cross-section. Using this approach, the formula (4) is transformed into:

$$\frac{\bar{q}_w}{St_0} = \left[\frac{1}{b} \cdot \frac{C_{p0}}{C_p} + \frac{1}{\Psi} \right]^{-1} \quad (5)$$

where $b = \frac{j_w}{\rho_0 \cdot U_0 \cdot St_0}$ is the permeability of the wall.

So far we have not accepted any suppositions, including anything about the flow pattern. Therefore the formula (5) is valid both for laminar and turbulent boundary layer.

Let us apply a linear approximation for the relative function of heat transfer

$$\Psi = 1 - \frac{b}{b_{cr}} \quad (6)$$

here b_{cr} is the critical value of injection parameter when $\Psi = 0$.

The approximation in form (6) was offered in [1,4], and the injection critical parameter for a laminar boundary layer was $b_{cr} \approx 1.86 \cdot (M'/M_0)^{1/3}$. Here M' and M_0 are the molecular masses for the gases of injected flow and main flow.

Fig. 1 exemplifies the calculations by (5) and (6) for the case of uniform injection $M' = M_0$; $b_{cr} = 1.86$. Here we also plotted the simulation results. With the growth in injection parameter, the heat flux first increases, then it reaches a maximum and then starts decreasing and vanishes at critical injection.

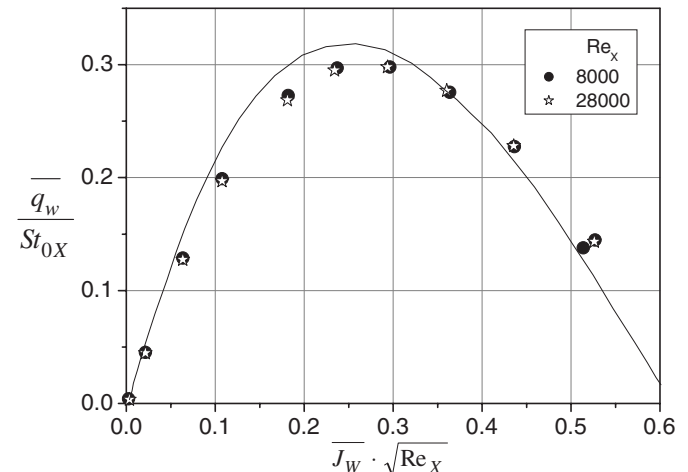


Fig. 1. Relative heat flux at uniform injection. Lines—calculated by (5) and (6). Dots—numerical simulation.

From the condition of maximum for function, $\bar{q}'_w(b) = 0$ we can obtain the corresponding value of injection parameter b^*

$$b^* = b_{cr} / \left(1 + \sqrt{\frac{C'_p}{C_{p0}} \cdot b_{cr}} \right) \quad (7)$$

For the case of uniform injection (Fig. 1) $C'_p = C_{p0}$ we obtain $b^*/b_{cr} \approx 0.42$, or $(\bar{j}_w \cdot \sqrt{Re_x})^* = (\bar{j}_w \cdot \sqrt{Re_x})_{cr} \cdot 0.42 = 0.62 \cdot 0.42 = 0.26$.

From relationships (5)–(7) we can estimate the possible value of maximal heat flux on a permeable wall:

$$q_w = St_0 \cdot \rho_0 \cdot U_0 \cdot C_{p0} \cdot (T_0 - T') \cdot \left[\frac{1}{b^*} \cdot \frac{C_{p0}}{C'_p} + \frac{1}{\Psi(b^*)} \right]^{-1} \quad (8)$$

Fig. 2 shows the simulation results for parameter's gradients on the porous wall. They are constructed in relative form:

$$\left(\frac{\partial U}{\partial y} \right)_w = \left(\frac{\partial U}{\partial y} \right)_w / \left(\frac{\partial u}{\partial y} \right)_w^{\max};$$

$$\left(\frac{\partial T}{\partial y} \right)_w = \left(\frac{\partial T}{\partial y} \right)_w / \left(\frac{\partial T}{\partial y} \right)_w^{\max}$$

Fig. 2 shows the results for uniform injection into the boundary layer for two kinds of boundary conditions: $T_w = \text{const}$ and $T' = \text{const}$. Naturally, the velocity gradients for both cases behave similar (they decrease monotonically with a higher injection). But the behavior of temperature gradients (the same-heat fluxes) are different: for the given temperature $T_w = \text{const}$ they behave like the velocity gradient, but at a given temperature of injected

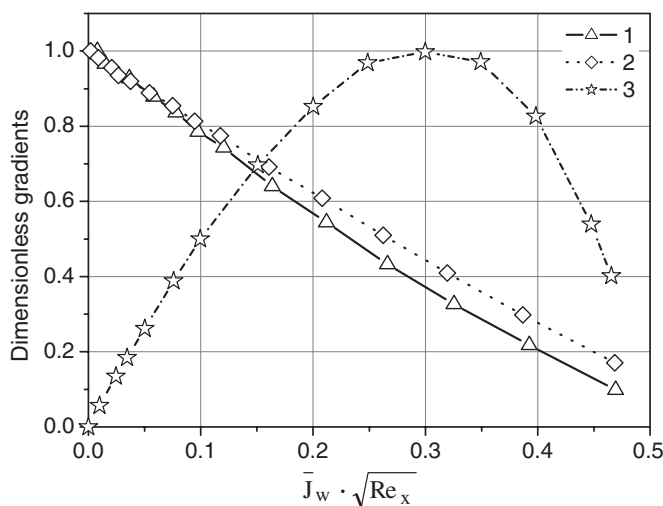


Fig. 2. Velocity and temperature wall gradients at uniform blowing normalized by their maximal values: (1) velocity gradient; (2) temperature gradient at $T_w = \text{const}$ and $T' = \text{const}$ conditions.

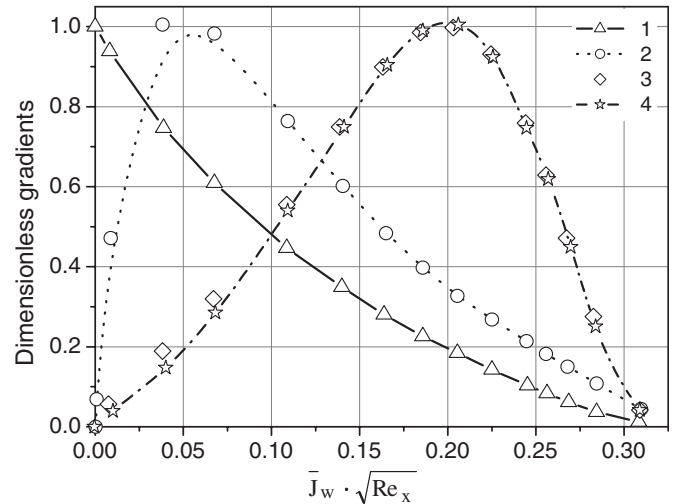


Fig. 3. Gradients of parameters on the wall normalized by their maximal values at helium injection into nitrogen: (1) velocity gradient; (2) temperature gradient; (3) enthalpy; (4) concentration.

gas $T' = \text{const}$ the wall temperature gradient first increases with injection parameter, then reaches the maximum and after that declines. Note that the mass concentration gradient as a function of injection (for $M' \approx M_0$) behaves in a similar way. It is interesting that if we relate those gradients to the parameter difference over the boundary layer

$$\left(\frac{\partial U}{\partial y} \right)_w / U_0; \quad \left(\frac{\partial T}{\partial y} \right)_w / (T_0 - T_w); \quad \left(\frac{\partial K}{\partial y} \right)_w / \Delta K$$

i.e., when we transform them into the form close to the definition of friction coefficient and Stanton number (thermal and diffusive), then all the gradients decline monotonically and almost coincide.

The simulation for wall gradients on the wall with injection of foreign gas (helium into nitrogen; $T_0 = 300$ K; $T' = 400$ K) is plotted in Fig. 3. We plotted the gradients for velocity and temperature, as well as for enthalpy and concentration. All these curves (the same as in Fig. 2) are treated in the relative format (related to maximal values). The wall gradients for temperature, enthalpy, and concentration exhibit maximums. It is interesting that the maximums of enthalpy gradient and concentration gradient occur at the same value of injection, but the maximum of temperature gradient occurs at much smaller injection. This means that the maximums of heat fluxes transported by thermal conductivity and diffusion take place at different values of injection.

2. Similarity between heat and mass transfer processes in boundary layers with variable content

In analysis of transfer processes in gaseous mixtures (for injection, evaporation, sublimation, combustion, etc.) the researchers often use the similarity between processes of heat and mass transfer, because this simplifies rather complex problems. Usually this requires some corrections

describing the influence of the Prandtl and Schmidt numbers [5–7]:

$$St_T = \frac{C_f}{2} \cdot \frac{1}{Pr^n}; \quad St_D = \frac{C_f}{2} \cdot \frac{1}{Sc^n} \quad (9)$$

where $\frac{C_f}{2}$, St_T , and St_D are the friction coefficient, thermal and diffusion variants of the Stanton numbers.

Experimental data and approximation of numerical solutions of energy equations suggest that exponent n for heat transfer at impermeable wall for the range of Prandtl number $0.3 < Pr < 15$ is $n = 2/3$ for laminar boundary layer, and $n = 0.6$ for turbulent boundary layer.

Experiments on evaporation and sublimation [8,9] and numerical solutions for diffusion equation at $j_w \rightarrow 0$ also demonstrated that for the Schmidt number in the range $0.3 < Sc < 15$ for laminar boundary layer $n = 2/3$, and for turbulent boundary layer $n = 0.6$. This is the basis [5,6] for analogy between heat and mass transfer in the form:

$$\frac{St_D}{St_T} = Le^n \quad (10)$$

here $Le = \frac{\rho \cdot D \cdot C_p}{\lambda} = \frac{Pr}{Sc}$ is the Lewis number.

By definition, the Lewis number characterizes the ratio between the heat transfer via diffusion and heat transfer via thermal conductivity. This paper presents an attempt to use the analysis of ratio of those kinds of wall heat flux for drawing of general conclusions about similarity of heat and mass transfer and influence of the Lewis number on those processes.

Consider a two-dimensional boundary layer in a gradientless flow in a binary gas mixture. The differential equations for energy and diffusion are written in the form:

$$\rho \cdot U \cdot \frac{\partial h}{\partial x} + \rho \cdot V \cdot \frac{\partial h}{\partial y} = \frac{\partial q}{\partial y} \quad (11)$$

$$\rho \cdot U \cdot \frac{\partial K_i}{\partial x} + \rho \cdot V \cdot \frac{\partial K_i}{\partial y} = \frac{\partial}{\partial y} \left(\frac{\mu}{Sc_i} \cdot \frac{\partial K_i}{\partial y} \right) \quad (12)$$

where K_i is the mass concentration of the i th component of mixture. The heat flux in gas mixture (if we neglect the thermal diffusion effects) is determined [10] by thermal conductivity and diffusional transfer of enthalpy:

$$\begin{aligned} q^\Sigma &= q_\lambda + q_D = -\lambda \cdot \frac{dT}{dy} + \sum j_i \cdot h_i \\ &= -\frac{\lambda}{C_p} \cdot \left[\frac{\partial h}{\partial y} + (Le - 1) \cdot \frac{\partial K'}{\partial y} \cdot (h' - h_0) \right] \end{aligned} \quad (13)$$

where h_0 and h' are the enthalpies for the main flow and injected gas in the specific point of boundary layer, $\overline{C_p}$ —heat capacity of a mix of gases. The energy equation in form (11) might be similar to the diffusion Eq. (12) under condition that $Le = 1$. In analysis of heat and mass transfer in boundary layers even if the Prandtl and Schmidt numbers are not equal one, it is often admitted that they are almost equal $Pr \approx Sc$ and so $Le \rightarrow 1$. It is also assumed that the ratio of similarity between coefficients of heat and mass transfer are fulfilled in the form (9) and (10).

With assumption $Le \rightarrow 1$, Leontiev [5] obtained the following formula:

$$St_\lambda = \frac{\left(-\lambda \cdot \frac{\partial T}{\partial y} \right)_w}{\rho_0 \cdot U_0 \cdot C_{p0} \cdot (T_w - T_0)} = \frac{\left(-\frac{\lambda}{C_p} \cdot \frac{\partial h}{\partial y} \right)_w}{\rho_0 \cdot U_0 \cdot (h_w - h_0)} = St_h \quad (14)$$

where $q_\lambda = \left(-\lambda \cdot \frac{\partial T}{\partial y} \right)_w = j_w \cdot C'_p \cdot (T' - T_w)$ (15)

and at $Le = 1$ $q_h = \left(-\frac{\lambda}{C_p} \cdot \frac{\partial h}{\partial y} \right)_w = q_\Sigma = j_w(h' - h_w)$ (16)

here $j_w = (\rho \cdot V)_w$ is the transversal mass flux on the wall; C'_p , T' , h' are the heat capacity, temperature and enthalpy of the injected gas; T_w and h_w are the wall temperature and gas enthalpy on the streamlined surface. Relation (14) for most cases is helpful for simplification of analysis of heat and mass transfer. Besides, it is very convenient for data treatment in case of injection of foreign gas through the porous surface—here we use temperature difference instead of enthalpy difference, and it not required to know the component concentrations on the wall, which is usually difficult in measurements. It is worth to note that for gases the range of the Prandtl number is much shorter than the range for the Schmidt number: for most cases we have $0.5 < Pr < 0.8$; $0.2 < Sc < 15$. The Lewis number might be quite different from one: $0.5 < Le < 3.5$. Besides, the numbers Sc and Le are concentration-dependent and the magnitudes may vary within the boundary layer.

Let us analyze the ratio between heat fluxes on the wall. Fig. 4 shows the balance of heat fluxes on a permeable wall. The heat transfer via thermal conductivity $q_\lambda = -\lambda \cdot (\partial T / \partial y)$ and diffusion $\sum j_i \cdot h_i$ may be directed either to one side or in opposite directions. Depending on the direction and magnitude of q_λ , we have the direction of the total heat flux q^Σ_w . Therefore, to avoid mistakes in the choice of q^Σ_w direction in making the heat valance on the wall, we wish to make it for condition when these fluxes are directed to one side (positive on “y” axis). The corresponding choice of parameters: $T' > T_0$; $C'_p > C_{p0}$. In general, it is not important for further analysis, because the signs of fluxes

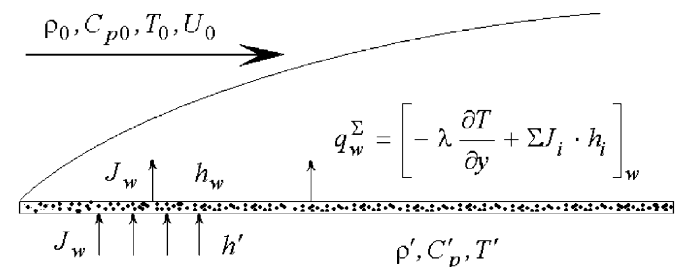


Fig. 4. Heat and substance fluxes balance on a wall.

are determined from the gradient of appropriate values. The balance on wall (Fig. 4) with account for (13) gives us

$$q_w^\Sigma = j_w \cdot (h' - h_w) = \left[-\lambda \cdot \frac{\partial T}{\partial y} + \sum j_i \cdot h_i \right]_w$$

$$= -\frac{\lambda}{C_p} \left[\frac{\partial h}{\partial y} + (Le - 1) \cdot \frac{\partial K'}{\partial y} \cdot (h' - h_0) \right]_w \quad (17)$$

The diffusion equation, written on the wall surface, takes the form:

$$(j_i)_w = (\rho \cdot V)_w \cdot (K_i)_w - \left(\rho \cdot D \cdot \frac{\partial K_i}{\partial y} \right)_w$$

or $\left(-\rho \cdot D \cdot \frac{\partial K'}{\partial y} \right)_w = j_w \cdot (1 - K')_w$ (18)

With this, the balance Eq. (17) is rewritten as

$$q_w^\Sigma = j_w \cdot (h' - h_w)$$

$$= \left[-\frac{\lambda}{C_p} \cdot \frac{\partial h}{\partial y} + \left(1 - \frac{1}{Le} \right) \cdot j_w \cdot (1 - K'_w) \cdot (h' - h_0)_w \right]_w \quad (19)$$

Using that $(1 - K') \cdot (h' - h_0)_w = h'_w - h_w$ we obtain

$$q_w^\Sigma = j_w \cdot (h' - h_w) = q_h + \left(1 - \frac{1}{Le} \right) \cdot j_w \cdot (h'_w - h_w) \quad (20)$$

here h_w and h'_w are the enthalpy for the mixture on the wall and the enthalpy for injected gas at wall's temperature.

Dividing this by q_w^Σ , we obtain the final relation:

$$\frac{q_h}{q_w^\Sigma} = \frac{St_h}{St_\Sigma} = 1 - \left(1 - \frac{1}{Le} \right) \cdot \frac{h'_w - h_w}{h' - h_w} \quad (21)$$

here: $St_h = \frac{\left(-\frac{\lambda}{C_p} \cdot \frac{\partial h}{\partial y} \right)}{\rho_0 \cdot U_0 \cdot (h_w - h_0)}$;

$$St_\Sigma = \frac{q_w^\Sigma}{\rho_0 \cdot U_0 \cdot (h_w - h_0)} \quad (22)$$

Note that according to formulas (14) and (22) we have three forms of thermal Stanton number: St_λ , St_h , St_Σ . For the case of injection of the same gas (or mixture of a steady composition) all three numbers are the same. But for injection of foreign gas, these numbers can be different. As one can see from Eq. (21), the difference between St_Σ and St_h depends on the Lewis number on wall, and these numbers are equal if $Le_w = 1$. That is for correct comparison of results on relative coefficients of heat transfer $\Psi = St/St_0 = f(b)$ (for injection of foreign gas) we must be aware that these numbers were calculated from the same form. It is very difficult to determine the value $\Psi = St_h/St_0$ from experiment, because this requires to know the enthalpy gradient on the wall.

Let us analyze the relation (21) on the example of most studied situation—helium injection into air, when the Le for the mixture varies in wide range. The calculation results for the heat flux ratio (or Stanton number) by formula (21)

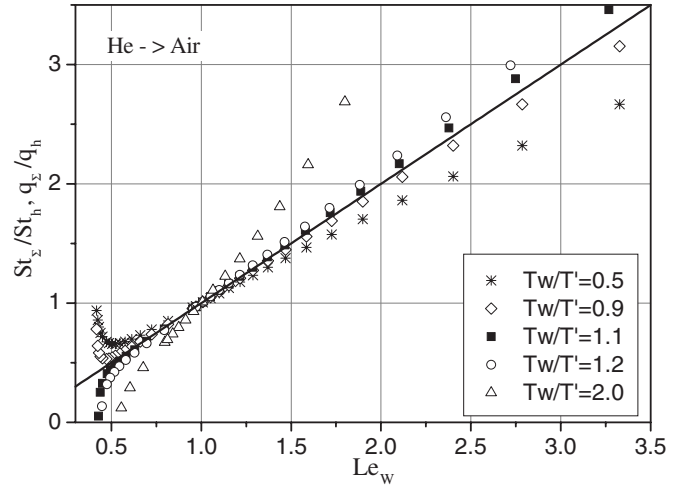


Fig. 5. Heat fluxes ratio q_w^Σ/q_h and Stanton numbers ratio St_Σ/St_h vs. Lewis number.

vs. the Lewis number on the wall are plotted in Fig. 5 for different temperature conditions.

If we assume that for the considered temperature interval the thermal capacity is independent of temperature, the last multiplier in formula (21) will take the form:

$$\frac{h'_w - h_w}{h' - h_w} = \frac{(C'_p - C_{pw}) \cdot T_w}{C'_p \cdot T' - C_{pw} \cdot T_w} \quad (23)$$

The we obtain from Eq. (21) under condition $T_w/T' \rightarrow 1$:

$$\frac{q_w^\Sigma}{q_h} = \frac{St_\Sigma}{St_h} \approx Le_w \quad (24)$$

This dependency in Fig. 5 is plotted as a straight line. The condition $T_w/T' \rightarrow 1$ corresponds to the conditions close to isothermal. The graph demonstrates a strong influence of the Lewis number and the temperature factor on the ratio q_Σ/q_h , which tends to one at $Le \rightarrow 1$.

The calculations by the same formula (21) vs. concentration of injected helium (on the wall) are plotted in Fig. 6. Note that assumption $Le = 1$ corresponds to condition $q_\Sigma = q_h$.

One can see from the figure that at certain conditions the total heat flux becomes zero (“pseudo-critical” injection) and then it changes the sign. Unlike the critical injection in the point with $q_\Sigma = 0$, here the condition $K'_w = 1$ and $T_w = T'$ are not fulfilled.

For injection of foreign gas, we see from formula (17) that heat fluxes driven by thermal conduction and diffusion may be co-directional or opposite. This depends on the relations between the temperatures and heat capacities of the main gas and injected gas. The condition $q_w^\Sigma = 0$ can be obtained only if these fluxes are opposite and $q_\lambda = -q_{diff}$.

The Eq. (17) gives us the conditions when $q_w^\Sigma = 0$:

$$\frac{T'}{T_w} = K'_w \cdot \left(1 - \frac{C_{p0}}{C'_p} \right) + \frac{C_{p0}}{C'_p} \quad (25)$$

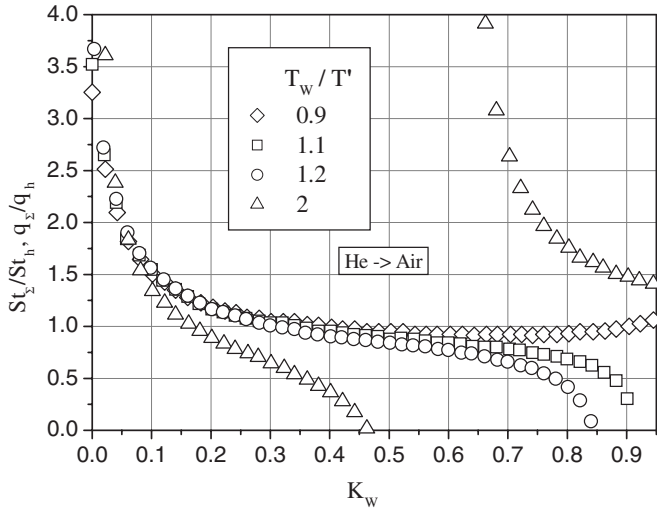


Fig. 6. Relative ratio for heat fluxes q_w^s/q_h and Stanton numbers St_s/St_h calculated by (21).

The relationship for enthalpy gradient gives us the condition on the wall $q_h = 0$:

$$\frac{T'}{T_w} - 1 = \frac{1}{Le_w} \cdot \left(\frac{C_{pw} - C'_p}{C'_p} \right) \quad (26)$$

At $Le \neq 1$ the transition points through zero for heat fluxes q_w^s and q_h might be not identical. This explains the anomalous behavior of dependencies in Fig. 6 for across direction of heat fluxes driven by thermal conductivity and diffusion.

Let us analyze the relation between the thermal and diffusion variants of Stanton numbers. If we take Eq. (13), when the heat transfer via thermal conductivity is much smaller than the diffusion contribution, and then use the definition for the diffusion-driven Stanton number $St_D = (-\rho \cdot D \cdot \frac{\partial K'}{\partial y})_w / \rho_0 \cdot U_0 \cdot \Delta K$ and all this gives us these relationships:

$$St_s = St_D \cdot \frac{h_w - (h_0)_w}{h_w - h_0}; \quad St_h = \frac{1}{Le_w} \cdot St_D \cdot \frac{h_w - (h_0)_w}{h_w - h_0} \quad (27)$$

One can see that this corresponds to the ratio (24).

For another limiting case, when the diffusion flux in Eq. (13) is negligible, we obtain:

$$q_w^s \Rightarrow q_h \Rightarrow q_\lambda; \quad St_s \Rightarrow St_h \Rightarrow St_\lambda \quad (28)$$

In this case this formula must be true: $St_s = St_h = Pr^{-n} \cdot C_t/2$, and for the diffusion problem we have $St_D = Sc^{-n} \cdot C_t/2$. This means the following ratio:

$$St_s = St_h = \frac{1}{Le^n} \cdot St_D \quad (29)$$

Calculations for relationships (27) and (29) for conditions close to isothermal $T_w/T_0 \rightarrow 1$ are plotted in Fig. 7. One can see from this figure that the ratio St_s/St_D may be in the range from 1 to $1/Le^{2/3}$ (for a laminar boundary layer $n = 2/3$). The ratio St_h/St_D is in a narrow range between

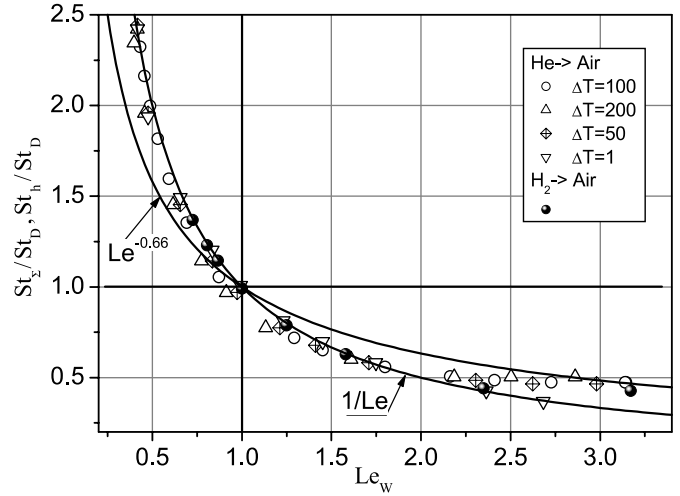


Fig. 7. The correlation between heat and diffusion Stanton numbers. Bold dots— H_2 injected into air, others— He injected into air.

curves $1/Le$ and $1/Le^{2/3}$. Then, by using (21), we can offer the following approximation for ratio between the coefficients of heat and mass transfer:

$$\frac{St_D}{St_s} = \frac{St_D}{St_h} \cdot \left[1 - \left(1 - \frac{1}{Le_w} \right) \cdot \frac{h'_w - h_w}{h' - h_w} \right] \quad (30)$$

where we can expect $St_D/St_h \approx Le_w^k$, and the exponent k varies from $k \approx n = 2/3$ to 1.

The points in Fig. 7 present the results of calculation for laminar boundary layer for helium and hydrogen injection into air in the form of relationship $St_h/St_D = f(Le_w)$. The most of points array for intensive injection ($Le_w \leq 2$; $K'_w \geq 0.03$) follow the dependency $St_D = St_h \cdot Le_w$, and at low injection ($Le_w > 2.5$; $K'_w < 0.03$) the calculations correspond to relation $St_D = St_h \cdot Le_w^{0.66}$. The $St_D = St_h \cdot Le_w$ relation was examined in [11] for the wet-bulb temperature calculating.

3. Peculiarities of a boundary layer with combustion

We have been carried out systematic study for a boundary layer with combustion, when the fuel evaporates from the surface or injected through a porous wall; some of our results were reported in [12–15].

The existence of a flame front causes a drastic (by factor of three and even more) fall in the coefficients of heat and mass transfer, and this is explained mainly by reduction of gas density in the high-temperature zone of reaction. The existence of heat release zone has a considerable impact on turbulent flow characteristics. Fig. 8 presents turbulence distributions over the boundary layer depth with and without combustion.

One can see that the pulsation level in the combustion zone decreases considerably. This suppression of turbulence is explained by a lower gas density and higher viscosity at the reaction front.

It is known that flow acceleration without combustion [16,17] also causes laminarization of the boundary layer and reduction in transfer coefficients. For an accelerated

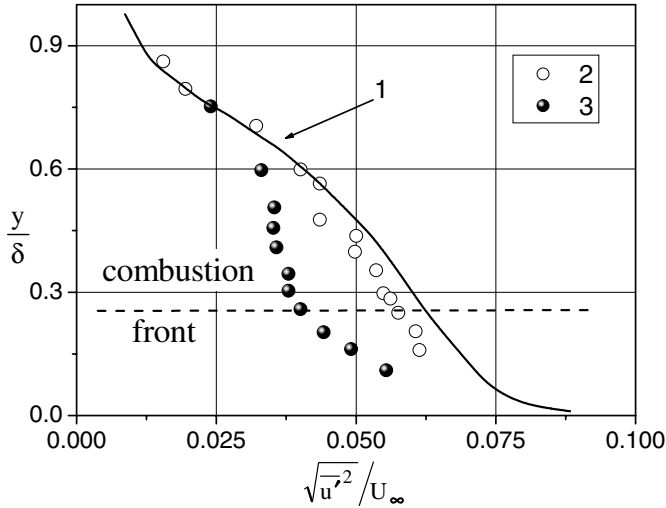


Fig. 8. The turbulence level in the boundary layer with and without combustion: (1) without combustion, Klebanoff's data; (2) without combustion; (3) with combustion.

boundary flow with combustion we expected the “doubled” effect of laminarization and further decrease in the transfer coefficients. Experiments [14] were carried out for a wide range of acceleration parameter:

$$k = \frac{v}{U_0^2} \cdot \frac{dU_0}{dx} \quad (31)$$

Instead of expected reduction in the coefficients of heat and mass transfer, we observed a considerable growth. This fact was explained after studying of the flow structure. For an accelerated flow, we observe a maximum of velocity profile in the zone of combustion front, and the flow resembles an “accelerated” near-wall jet. This means that the flow acceleration in the front zone is higher than in the mainstream; a kind of “shooting” occurs in the flame front. This is explained by rather simple reasoning. If we accept a supposition that in the differential equation of motion $(\frac{\partial x}{\partial y})^* \ll \frac{\partial P}{\partial x}$ and with account for maximum in the velocity profile inside the combustion front, meaning that $(\frac{\partial U}{\partial y})^* = 0$, we obtain for the front zone, at $y = y^*$, the following equation:

$$\rho_* \cdot U_* \cdot \frac{dU_*}{dx} = - \frac{dP}{dx} \quad (32)$$

where * stands for parameters in the flame front.

Beyond the boundary layer:

$$- \frac{dP}{dx} = \rho_0 \cdot U_0 \cdot \frac{dU_0}{dx} \quad (33)$$

The relationship for the acceleration parameter (31)

$$\frac{dU_0}{U_0^2} = \frac{k}{v_0} \cdot dx \quad (34)$$

and at $k = \text{const}$

$$\frac{U_0}{U_S} = [1 - k \cdot Re_x]^{-1} \quad (35)$$

where $Re_x = \frac{U_S x}{\nu}$ and $U_S = U_0$ are in the initial cross-section.

With account for the state equation, we obtain from these formulas the relation for the velocity in the flame front, at $M^* \approx M_0$:

$$\frac{U_*}{U_S} = \sqrt{\frac{T_*}{T_0}} \cdot \sqrt{\frac{1}{(1 - k \cdot Re_x)^2} + \frac{T_0}{T_*} - 1} \quad (36)$$

Fig. 9 presents comparison of calculations and experiment.

Note that several points were obtained at a higher turbulence. A special research was performed on study of flow turbulence on the parameters of the boundary layer with combustion of ethanol, which evaporates from the wall. With the growth of turbulence degree, the high-temperature area in the zone of reaction front “blurs” and the maximal temperature decreases (Fig. 10). The temperature gradient at the wall increases, i.e., the reaction front shifts towards the wall.

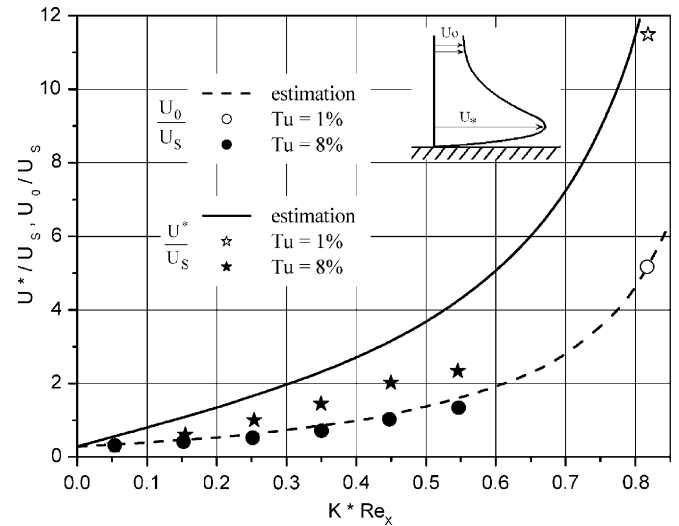


Fig. 9. Flow acceleration in the boundary layer with combustion.

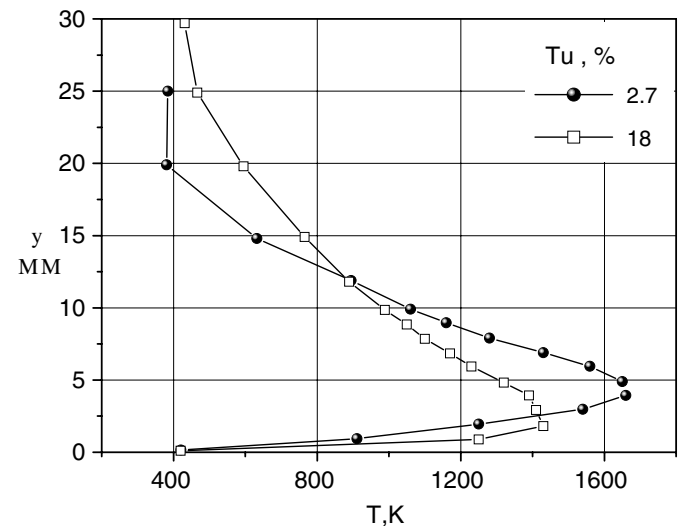


Fig. 10. Influence of flow turbulence on temperature distributions in the boundary layer with combustion. $U_0 = 10 \text{ m/s}$; $x = 140 \text{ mm}$.

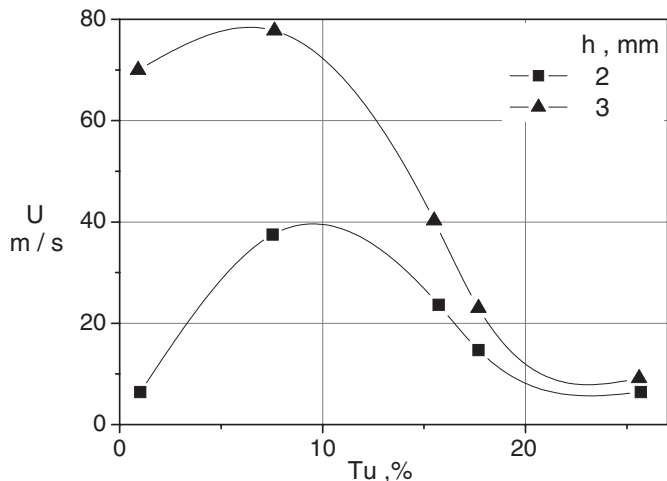


Fig. 11. Influence of flow turbulence on flame-out velocity in the boundary layer with diffusion-driven combustion of evaporating ethanol.

The effect of flow turbulence on the flame blow-off velocity (critical air flow velocity that causes a flame-out) is shown in Fig. 11. Here h is the rib height in the initial cross-section. The rib here is a flame holder for combustion of ethanol evaporating from a porous surface.

Our idea before those experiments was that the growth in the air mainstream turbulence should lead to intensification of the mixing process and through that to a lag in flame-out. However, as apparently may be seen from Fig. 11, in the presented case the increase of turbulence results decreases drastically the flame-out velocity.

Obviously, one of possible explanation is that with a growth in turbulence the flame front displaces to the wall (see Fig. 10). But during combustion above the surface with evaporation, the flame front cannot descent to the wall because the wall temperature cannot be higher than the boiling temperature of evaporating fuel.

Acknowledgement

This work was supported by RFBR grant 05-02-16478 and RF Presidents grant NSH-816.2003.8.

References

- [1] J.F. Gross, J.P. Hartnet, J.D. Masson, C.A. Gazley, A review of binary laminar boundary layer characteristics, *Int. J. Heat Mass Transfer* 3 (1961) 198–221.
- [2] R.B. Landis, A.F. Mills, The calculation of turbulent boundary layers with foreign gas injection, *Int. J. Heat Mass Transfer* 15 (1972) 1905–1932.
- [3] E.M. Sparrow, E.R. Eckert, V.Zh. Minkovich, Thermodynamic relationship between processes of heat and mass transfer in collection, in: A.V. Lykov (Ed.), *Heat and Mass Transfer*, Minks, vol. 2, 1965, pp. 27–45.
- [4] A.I. Leontiev, *Heat transfer in laminar boundary layer*, Textbook for MHTU Students, MHTU Izdatelstvo, Moscow, 1977.
- [5] A.I. Leontiev (Ed.), *Theory of Heat and Mass Transfer*, MHTU Izdatelstvo, Moscow, 1997.
- [6] D.B. Spalding, *Convective Mass Transfer*, Energia, Moscow-Leningrad, 1965.
- [7] V.Y. Likhushin, *Heat Transfer Theory*, Keldysh Centre, Moscow, 1998.
- [8] E.R. Eckert, R.M. Drake, *Theory of Heat and Mass Transfer*, GEI, Moscow, 1961.
- [9] B.S. Petukhov, *Heat Transfer in Moving Uniform Medium*, MEI, Moscow, 1993.
- [10] L. Leeze, *Convective heat transfer for case of substance supply and chemical reactions*, coll., *Gas Dynamics and Heat Transfer with Chemical Reactions*, Izdatelstvo IL, Moscow, 1962.
- [11] V.V. Lukashov, On the determination of the surface temperature of an evaporating liquid, *Theor. Found. Chem. Eng.* 37 (4) (2003) 351–355.
- [12] B.F. Boyarshinov, E.P. Volchkov, V.I. Terekhov, Structure of boundary layer with blowing and combustion of ethanol, *Combust. Explo. Shock Waves* 28 (3) (1992) 235–242.
- [13] B.F. Boyarshinov, E.P. Volchkov, V.I. Terekhov, Heat and mass transfer in a boundary layer with the evaporation and combustion of ethanol, *Combust. Explo. Shock Waves* 30 (1) (1994) 7–14.
- [14] B.F. Boyarshinov, E.P. Volchkov, V.V. Lukashov, Heat transfer in accelerated reacting boundary layer, *Dokl. Energetica* 32 (6) (1996) 763–765.
- [15] E.P. Volchkov, V.I. Terekhov, V.V. Terekhov, Boundary-layer structure with hydrogen combustion with different injection intensities, *Combust. Explo. Shock Waves* 38 (3) (2002) 269–277.
- [16] R.J. Moffat, W.M. Kays, *A Review of Turbulent—Boundary Layer Heat Transfer Research at Stanford 1958–1983*, *Advances in Heat Transfer*, vol. 16, Academic Press, Inc., 1984, pp. 242–365.
- [17] P.S. Roganov, V.P. Zabolotsky, E.V. Shishov, A.I. Leontiev, Some aspects of turbulent heat transfer in accelerated flows on permeable surfaces, *Int. J. Heat Mass Transfer* 28 (8) (1984) 1251–1259.